

## X-ray-absorption near-edge-structure study of $\text{La}_{2-x}(\text{Ba,Sr})_x\text{CuO}_{4-y}$ superconductors

J. M. Tranquada, S. M. Heald, and A. R. Moodenbaugh

*Brookhaven National Laboratory, Upton, New York, 11973*

(Received 5 June 1987)

Superconductors with the composition  $\text{La}_{2-x}(\text{Ba,Sr})_x\text{CuO}_{4-y}$  and  $x=0.0$  to  $0.3$  have been studied through measurements of x-ray-absorption near-edge structure at the Cu  $K$  and La  $L$  edges. Contrary to recent band-structure calculations, we find that the Cu  $3d$  electrons are localized with the copper ions having an integral  $3d^9$  configuration ( $2+$  valence) independent of dopant concentration. Variation in the area of the "white lines" at the La  $L_{2,3}$  edges with doping indicates that reduction of the valence charge results in an increase in unoccupied states (probably consisting of holes in the O  $2p$  band) having  $d$  symmetry relative to the La site. These O  $2p$  holes also appear to have  $d$  symmetry with respect to the Cu sites.

### I. INTRODUCTION

The discovery by Bednorz and Müller<sup>1</sup> of a new class of superconducting oxides with high transition temperatures ( $T_c$ ) has been followed by rapid progress in the identification and purification of several new high- $T_c$  superconducting compounds.<sup>2-12</sup> The original work<sup>1</sup> on the La-Ba-Cu-O system has led to the study of the system<sup>2-7</sup>  $\text{La}_{2-x}\text{A}_x\text{CuO}_{4-y}$  with  $A = \text{Ba, Sr, Ca}$ , and the system<sup>8-12</sup>  $\text{RBa}_2\text{Cu}_3\text{O}_{9-y}$  with  $R$  almost any rare-earth element. A common and apparently key feature among these perovskitelike compounds is the presence of two-dimensional layers containing only Cu and O atoms. The electronic structure near the Fermi energy in these systems is derived predominantly from Cu  $3d$  and O  $2p$  states. Another important factor is that the total count of valence electrons is less than that required to give each of the component ions its standard formal valence. Assuming valences of  $3+$  for La, Y, and R,  $2+$  for Ba, Sr, and Ca, and  $2-$  for O, that fact is sometimes expressed by saying that some of the Cu atoms must have a valence of  $3+$  instead of the more common  $2+$ .

A great deal of effort is presently being devoted to the study of the 90-K superconductors  $\text{RBa}_2\text{Cu}_3\text{O}_{9-y}$ . However, for studying the superconducting mechanism in this class of oxides, the  $\text{La}_{2-x}(\text{Ba,Sr})_x\text{CuO}_{4-y}$  system has the advantage that, through the doping variable, one can continuously vary the number of valence electrons. The extra variable is an important one for experimentally testing theories of electronic structure and superconductivity.

As mentioned previously, an important feature of the superconducting oxides is their anisotropic crystal structure. The Sr- and Ba-doped compounds have a layered, tetragonal structure containing planes of Cu atoms surrounded by corner-sharing oxygen octahedra.<sup>13</sup> The La (and Sr or Ba) atoms sit in layers between the Cu planes. In the undoped material, neighboring octahedra along a (110) direction are slightly tilted in opposite directions with respect to the  $c$  axis, resulting in a larger, orthorhombic unit cell.<sup>13,14</sup>

Several band-structure calculations have recently appeared<sup>15-17</sup> for the high-temperature tetragonal phase of  $\text{La}_2\text{CuO}_4$ . The results of these calculations appear to be

quite similar and have been extrapolated to the Sr- and Ba-doped superconductors in order to interpret the mechanism behind the superconductivity. The generally agreed upon scenario is as follows.<sup>13,15-17</sup> The  $3d_{x^2-y^2}$  orbital of a Cu atom hybridizes strongly with the  $2p_{x,y}$  states of its oxygen neighbors in the basal plane. Of the three bands formed, the topmost one is exactly half filled in the undoped compound. Because of the two dimensionality of the valence bands, the Fermi surface shows almost perfect nesting, and as a result, a Peierls distortion should occur, resulting in a gap at the Fermi level and, thus, explaining the semiconducting behavior of the undoped material. Doping lowers the Fermi energy and reduces the degree of Fermi-surface nesting so that the undistorted structure is stable. However, reduced nesting still causes a very large electron-phonon coupling which presumably explains the high  $T_c$ .

As alternatives to the conventional electron-phonon interaction, several electron-electron pairing mechanisms have been presented. Anderson<sup>18,19</sup> has suggested a "resonating-valence-bond" (RVB) model in which the electrons in the top valence band are localized in fluctuating, antiferromagnetically coupled pairs. The resonating bonds do not have crystalline order and can move about when the exactly half-filled band condition in  $\text{La}_2\text{CuO}_4$  is removed by doping. Kivelson, Rokhsar, and Sethna<sup>20</sup> find that stabilization of the RVB state relative to an ordered Néel state may require a coupling of a bond pair to a lattice distortion which shortens the corresponding Cu-O bond length.

Lee and Ihm<sup>21</sup> have considered the possibility that the strong electron-electron correlations cause the copper  $3d_{z^2}$  band to be lifted to the Fermi energy, resulting in interband scattering mediated by phonons and plasmons. On the other hand, Varma, Schmitt-Rink, and Abrahams<sup>22</sup> ignore the correlation energy and propose that charge transfer excitations may be important, with the copper ions fluctuating between  $\text{Cu}^{1+}$ ,  $\text{Cu}^{2+}$ , and  $\text{Cu}^{3+}$ .

The model which will be shown to be the most consistent with our results is one developed by Emery.<sup>23</sup> Starting from an extended Hubbard model, he has shown that, for a reasonable range of model parameters, each copper site should have a single  $d$  hole. Because of the

Hubbard gap at the Fermi energy, doping leads to holes in the O  $2p$  band with no change in occupation of the Cu  $3d$  states. Superconductivity results from pairing of the O  $2p$  holes via exchange interactions.

The band-structure calculations predict that the Cu  $3d$  electrons are itinerant, while other models assume that they are localized, perhaps with fluctuating valence. To learn about the actual valence charge distribution, we have studied the x-ray-absorption near-edge structure (XANES) measured at the Cu  $K$  and La  $L$  edges in  $\text{La}_{2-x}\text{Sr}_x\text{CuO}_{4-y}$  and  $\text{La}_{2-x}\text{Ba}_x\text{CuO}_{4-y}$  for  $x=0$  to 0.3. Following a description of sample characterization and experimental procedure, a discussion of valence determination from Cu  $K$ -edge measurements is given. Absorption spectra obtained for the layered-perovskite samples are compared with measurements on a number of reference materials, and it is shown that the Cu ions have a  $3d^9$  configuration in  $\text{La}_{2-x}(\text{Ba},\text{Sr})_x\text{CuO}_{4-y}$ , independent of  $x$ . Next we discuss the La  $L_{2,3}$ -edge measurements, which indicate that the number of La  $5d$  and/or O  $2p$  holes increases with doping. Finally, the implications of these results for various models of the electron-pairing mechanism are discussed. A brief description of this work has been published previously.<sup>24</sup>

## II. EXPERIMENTAL PROCEDURE

### A. Sample preparation and characterization

The samples were prepared from powders of the following materials:  $\text{La}_2\text{O}_3$  (G. F. Smith 99.99%, Aesar 99.99%), CuO (MCB reagent grade ground and oxidized at 800°C, Aesar 99.999%), and  $\text{BaCO}_3$  (reagent grade, Aesar 99.99%), or  $\text{SrCO}_3$  (reagent grade). The components were mixed in the appropriate proportions, ground together, and fired in air at 1000–1100°C. (The  $\text{La}_2\text{O}_3$  was dried at 800°C in air for at least four hours prior to weighing and mixing.) After a second grinding, pellets were formed and fired in air at 1100°C. Some of the samples were fired a third time at 900–1100°C in air or oxygen. The crystal structures of the samples were checked with x-ray diffraction. All samples had the expected  $\text{K}_2\text{NiF}_4$ -type structure (with orthorhombic distortion for  $\text{La}_2\text{CuO}_4$ ). The content of impurity phases is generally less than 5%, with no observable impurities above ~2% in some cases.

The superconducting properties were characterized by measuring the change in ac magnetic susceptibility with temperature. The transition temperature, as determined by the position of the initial sharp drop in susceptibility, is listed for each sample in Table I. A qualitative measure of the sample fraction showing superconductivity is also indicated. (Determination of the superconducting fraction from the ac susceptibility signal strength is possible in this case because of the inhomogeneous nature of the samples. Experimental evidence<sup>25</sup> indicates that the small superconducting grains are separated by layers of normal material.)

Reference compounds  $\text{Cu}_2\text{O}$ , CuO,  $\text{Cu}(\text{OH})_2$ , and  $\text{CuFe}_2\text{O}_4$  were obtained from Alfa. A sample of  $\text{Cu}^{1+}$  ions in solution was prepared by electrolytically dissolving

TABLE I. Information on samples studied, including nominal dopant concentration, superconducting transition temperature, and fraction of sample showing superconductivity.

Sample	Dopant	$x$	$T_c$ (K)	Superconducting fraction
1		0.00		
2	Sr	0.10	29	Moderate
3	Sr	0.15	38	Large
4	Sr	0.20	29	Large
5	Sr	0.30	37	Very small
6	Ba	0.15	28	Large
7	Ba	0.20	14	Small
8	Ba	0.30	30	Very small

Cu metal into an aqueous solution of HCl. A solution containing  $\text{Cu}^{2+}$  ions was prepared by dissolving  $\text{CuCl}_2$  in water.

### B. X-ray absorption measurements

The x-ray-absorption measurements were performed on beam line X-11A at the National Synchrotron Light Source using a Si(111) double-crystal monochromator. The nominal energy resolution at 9 keV was ~1.3 eV for near-edge-only scans and ~2.4 eV for scans including the extended fine structure. Each of the samples was ground to a fine powder and rubbed onto tape; Kapton was used for samples measured at low temperature and Scotch Magic tape for room temperature only. The number of tape layers used was adjusted to give an edge step  $\Delta\mu x$  of less than 1.5 (except for CuO and  $\text{Cu}_2\text{O}$ , which had a somewhat larger step size) at the Cu  $K$  edge and less than 1.0 at the La  $L_3$  edge. For the temperature-dependent measurements, the powder-on-tape samples were mounted on a copper sample holder and cooled with an Air Products Displex refrigerator. Temperatures were monitored with a gold-chromel thermocouple attached to the sample holder.

As the energy calibration of the monochromator can drift due to shifts in the position of the electron beam in the storage ring or due to temperature changes in the monochromator crystals, the energy scale for each Cu  $K$ -edge measurement was referenced to a simultaneous Cu foil measurement. With this method, the relative positions of edges were determined with an accuracy of  $\pm 0.1$  eV.

## III. Cu $K$ EDGE

### A. A question of valence

The problems of specifying and determining valence are difficult ones. Chemists define a formal valence equal to the minimum number of electrons which must be added to or removed from an atom to achieve a closed-shell, rare-gas configuration. Physicists who calculate electronic structure sometimes attempt to calculate the amount of valence charge within a muffin-tin sphere (whose radius is not uniquely defined). The valence measured by the posi-

tion of an x-ray-absorption edge is something else again. In the x-ray-absorption measurement, the position of an edge is equal to the difference in energy between the initially unexcited atom sitting in the solid, and a final state consisting of the same atom with a core hole plus a photoelectron in the lowest-energy unoccupied state of appropriate symmetry, as determined by the dipole selection rule. (We ignore for the moment excitations involving two electrons.) For a  $K$  edge, the core hole is a  $1s$  state and the photoelectron has  $p$  symmetry with respect to the absorbing atom. If we somehow remove a valence electron from the atom, the effective potential seen by the initial  $1s$  and the  $p$  symmetry final state will change. The change in the transition energy, due to the removal of an electron, is approximately equal to the difference in the energy shifts of the two states due to the screening change.<sup>26</sup> The size of the screening change seen by the two states depends on the angular momentum and energy of the electron removed.

To better understand the relationship between absorption edge shifts and valence, we have performed a series of atomic calculations.<sup>27</sup> The x-ray-absorption transition energy for a Cu atom was calculated as the difference between the total energy of the ground state and the energy of a final state with an electron transferred from a  $1s$  to a  $4p$  state. Transitions to a  $3d$  final state were also calculated in those cases where there is a  $3d$  hole in the ground state. (The  $1s \rightarrow 3d$  transition is dipole forbidden but quadrupole allowed, so that it will be very weak compared to  $1s \rightarrow 4p$ .) These calculations were repeated for several different valence configurations. The resulting transition energies, referenced to the zero valence  $1s \rightarrow 4p$  energy, are listed in Table II. As can be seen from the table, removing a  $4s$  electron causes a 3-eV edge shift, while removing a  $3d$  electron results in a 10-eV shift. Hence, the shift in  $E(1s \rightarrow 4p)$  is not a linear function of the number of electrons removed.

In a solid, the actual net charge within an atomic sphere will be somewhere between the formal valence for the ion and zero. The extra-ionic charge, in the case of a positive ion, will have some screening effect on the atomic energy levels and, hence, may shift x-ray transition energies from their free ion values. To get an extreme estimate of the effects of such screening, we have repeated the atomic cal-

culations for the series of formal valences, but with the ionic charge neutralized by the addition of an appropriate number of  $4p$  electrons. While the screening effects are significant, the edge shift due to removing a  $3d$  electron is still 7–8 eV. The actual amount of screening charge in a solid would probably be considerably less than that considered here. In any case, it is clear that the absence or presence of  $3d$  and  $4s$  electrons is much more important for determining the edge position than any extra charge contributed by neighboring anions.

The Cu  $4p$  final-state shifts predicted by the calculations may seem quite large compared to the net edge shifts commonly observed at transition-metal  $K$  edges. To check the validity of comparing atomic calculations with experiment, we have repeated the calculations for a neutral Sm atom with different numbers of  $4f$  electrons. Changing the valence electron configuration for the Sm atom from  $4f_{5/2}^6 5d_{3/2}^0 6s^2$  to  $4f_{5/2}^5 5d_{3/2}^1 6s^2$  causes a shift in the  $2p_{3/2} \rightarrow 5d_{3/2}$  transition ( $L_3$  edge) of 6.2 eV, in good agreement with the experimentally observed<sup>28</sup> shift of  $\sim 7$  eV between  $L_3$  edges for  $\text{Sm}^{2+}$  and  $\text{Sm}^{3+}$ .

The near-edge spectrum of an atom, whether in a gas, liquid, or solid, is dominated by a sharp jump in absorption due to the onset of transitions to continuum states; the jump is smoothed somewhat by core-hole lifetime effects. Transitions to localized levels are superimposed on the edge jump. If the energy of an atomlike final state falls below the continuum threshold, a narrow absorption feature may be observed. In ionic systems, the potential due to neighboring ions may enhance the binding energy of such a final state. On the other hand, if the energy overlaps the continuum spectrum, an atomlike final state may broaden into a resonance feature.

In a solid, of course, the valence- and conduction-electron states lose some of their atomic character due to hybridization with states on neighboring atoms. In metallic and strongly covalent materials, the electronic bands which form can be quite broad. The final states for  $K$ -edge absorption need not be formed from atomic  $p$  states—they can involve any linear combination of atomic states in the solid having  $p$  symmetry with respect to the absorbing atom. Strong hybridization can smear the energies of  $p$ -symmetry final states over a wide range, and, thus, cause the energy position of the initial strong absorption feature at an edge to be shifted to significantly lower energy than one would predict from an atomic calculation.

In an ionic compound, on the other hand, hybridization effects are relatively small and valence electrons are more localized. For insulators, there are no free electrons available to screen the core hole created by an x-ray-absorption event. As a result, we expect that atomlike photoelectron final states will appear as strong resonances since such states can effectively screen the core hole and also have a relatively large overlap with the initial state. In an insulating Cu compound, the first strong absorption feature should correspond to a Cu  $4p$ -like resonance with an energy close to that calculated for an isolated ion. Note that any Madelung potential due to the ionic environment has no effect on the transition energy for a localized final state since the transition energy is equal to the difference between initial- and final-state energies.

TABLE II. Calculated  $1s \rightarrow 4p$  and  $1s \rightarrow 3d$  transition energies for several valences of Cu. The energies are given relative to the zero valence value.

Formal valence	Screened	Valence configuration	$E(1s \rightarrow 3d)$ (eV)	$E(1s \rightarrow 4p)$ (eV)
0		$3d^{10}4s$		0.0
+1	no	$3d^{10}$		2.6
+1	no	$3d^9 4s$		8.6
+2	no	$3d^9$	-6.4	11.7
+3	no	$3d^8$	-4.7	22.6
+1	yes	$3d^{10}4p$		1.1
+2	yes	$3d^9 4p^2$	-6.6	7.8
+3	yes	$3d^8 4p^3$	-5.5	15.8

In certain cases, such as a cationic absorber in an insulator, the interaction between the core hole and a low-energy photoelectron combined with the potential due to neighboring anions, may result in an exciton—a localized, bound final state with an energy in the forbidden gap. The energy of the exciton may be several volts lower than the corresponding free-ion state, and its intensity is generally enhanced due to the localization. Even if an atom-like final state is not quite bound, it may exhibit excitonic enhancement of its intensity and a shift to lower energy. Such an effect can cause some difficulties when one attempts to associate edge features with valence.

Another complication in determining valence comes from the fine structure due to interference effects in the final state caused by scattering of the photoelectron by neighboring atoms. The fine structure depends on the numbers of, types of, and radial distances to neighboring atoms, and, hence, will vary for different crystal structures. As demonstrated by Bunker and Stern<sup>29</sup> in the case of  $\text{KMnO}_4$ , the scattering fine structure extends down to the continuum threshold. In attempting to determine valences from real absorption edge measurements, one must try to separate atomic features from fine-structure effects.

To summarize the discussion in this section, atomic calculations indicate that the addition or removal of a  $3d$  electron in a copper atom causes a shift in the  $1s \rightarrow 4p$  transition of approximately 10 eV. Changing the occupation of a  $4s$  or  $4p$  state by unity results in a shift of only  $\sim 2$  eV. Nonintegral  $3d$  occupancy, as expected for itinerant electrons in a solid, can result in a continuous variation in edge position. In an ionic compound with localized  $3d$  electrons, we expect the relative position of the first strong absorption feature to correspond to the energy obtained from the free-ion calculations. However, excitonic- and fine-structure effects must be considered when attempting to identify atom-like features in XANES.

### B. Reference compounds

Reference materials containing Cu atoms with several different valences have been measured. To understand the relevance of the measurements, a brief description of the materials will be given. Pure copper is metallic, with a nominal  $3d^{10}4s^1$  valence configuration.  $\text{Cu}_2\text{O}$ ,  $\text{CuO}$ , and  $\text{CuFe}_2\text{O}_4$  are semiconductors,<sup>30–32</sup> with  $\text{CuO}$  exhibiting antiferromagnetic ordering of the Cu  $3d$  spins below 230 K.<sup>31</sup> We assume that  $\text{Cu}(\text{OH})_2$  is also an insulator. The expected Cu valence configurations and some structural information for the oxides are summarized in Table III. In  $\text{Cu}_2\text{O}$ , copper is linearly coordinated by a pair of oxygen ions, while in the other compounds each copper atom is surrounded by a tetragonally distorted octahedron of oxygens. It is generally accepted that the distortion is due to the Jahn-Teller instability of the  $\text{Cu}^{2+}$  ion. For the aqueous solutions of  $\text{CuCl}$  and  $\text{CuCl}_2$ , the Cu ions should have  $3d^{10}$  and  $3d^9$  configurations corresponding to  $1+$  and  $2+$  valences, respectively. Although some ordering of anions about the Cu cations may occur,<sup>33,34</sup> the important thing is that interatomic interactions should be almost exclusively ionic.

TABLE III. Formal valence and expected valence configuration of Cu ions, and coordination numbers  $N$  and interatomic distances  $R$  of oxygen neighbors in several reference compounds.

Compound	Formal valence	Valence configuration	$N$	$R$ (Å)
$\text{Cu}_2\text{O}$	+1	$3d^{10}$	2	1.85
$\text{CuO}$	+2	$3d^9$	2	1.95
			2	1.96
			2	2.78
$\text{CuFe}_2\text{O}_4$	+2	$3d^9$	4	2.01
			2	2.14
$\text{Cu}(\text{OH})_2$	+2	$3d^9$	2	1.93
			2	1.94
			2	2.63
$\text{La}_2\text{CuO}_{4-y}$	+2	$3d^9$	4	1.90
			2	2.43

The situation for  $\text{CuFe}_2\text{O}_4$  is actually somewhat more complicated than implied above. The structure of this compound, known as an “inverse spinel,” contains both octahedral and tetrahedral cation sites, with copper ions sitting predominantly on octahedral sites and iron atoms split between the two. The parameters listed in Table III are for Cu atoms in octahedral sites only. X-ray diffraction measurements<sup>35</sup> at room temperature show, however, that approximately 10% of the copper atoms sit in tetrahedral sites, and theory<sup>36</sup> suggests that the tetrahedrally coordinated copper ions should have a  $1+$  valence. It follows that we should expect to see a mixture of approximately 90%  $\text{Cu}^{2+}$  and 10%  $\text{Cu}^{1+}$ .

Cu  $K$  edges measured in Cu metal,  $\text{Cu}^{1+}$  ions in solution,  $\text{Cu}_2\text{O}$ , and  $\text{Cu}^{2+}$  ions in solution are displayed in Fig. 1. A straight line was fit to the region  $-200$  to  $-50$  eV below the edge, extrapolated through the edge, and subtracted. The absorption thickness has been normalized to a step height  $\Delta\mu x$  of 1 by fitting a straight line to the region 100 to 300 eV above the edge, extrapolating back to the edge, and taking the height at the edge as the step height. (A similar procedure has been applied to all of the XANES data presented in this paper.) The zero of energy has been taken as the position of the first bump on the edge for Cu metal.

The first point to be made is that for all four examples, the midpoint of the main absorption jump occurs at approximately 5–7 eV. The continuum threshold shifts very little, if at all, in going from one system to the next. What we wish to concentrate on is the first strong absorption feature in each case.

Since pure Cu is metallic, the  $4p$  states are spread out into broad bands due to hybridization with  $4s$  and  $3d$  states. As discussed in the last section, we assume that the position of the first bump on the edge is at somewhat lower energy than one would expect for the  $4p$  state in a neutral, isolated copper atom. The conduction electrons provide good screening and eliminate any atom-like resonances. Indeed, it has been shown that the entire near-edge region can be accurately simulated by a single-scattering fine-structure calculation.<sup>37</sup>

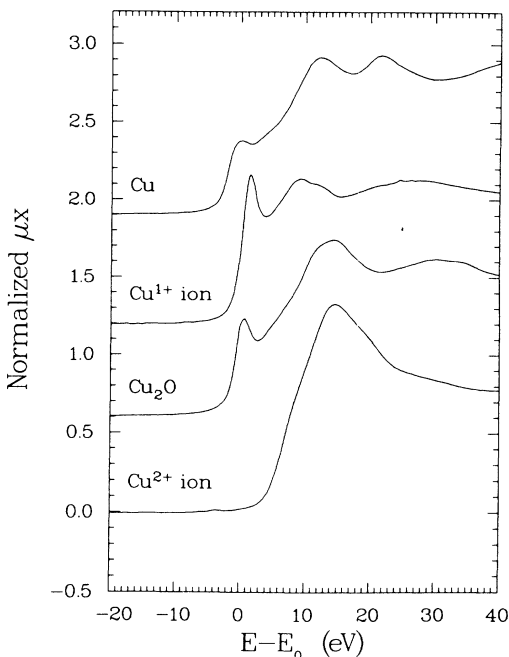


FIG. 1. Normalized near-edge structure measured at the Cu  $K$  edge in several copper reference systems discussed in the text. The curves have been shifted vertically for clarity, and  $E_0 = 8980$  eV.

For the reference compounds having a formal copper valence of  $1+$  (the semiconductor  $\text{Cu}_2\text{O}$  and the  $\text{Cu}^{1+}$  ions in solution), we expect that the Cu valence configuration is  $3d^{10}$ , that the initial absorption feature should correspond to an atomic  $4p$ -like state, and that it should be shifted  $\gtrsim 2$  eV to higher energy relative to the first peak of Cu metal. It is observed, however, that the first peak in both cases is quite sharp, located below the continuum threshold, and shifted by only 0.5 eV for  $\text{Cu}_2\text{O}$  and 1.5 eV for  $\text{Cu}^{1+}$  ions. The sharpness of this feature and its low energy are consistent with excitonic enhancement of the atomic  $4p$  final state. Indeed, very intense  $s$ -symmetry excitons have been observed in  $\text{Cu}_2\text{O}$  at the Cu  $L_{2,3}$  edges by Hulbert, Bunker, Brown, and Pianetta.<sup>38</sup> Resonant  $s$  and  $p$  excitons had previously been predicted by Robertson.<sup>39</sup> Even without excitonic enhancement, the initial  $4p$ -like feature is sharp because it falls in the forbidden gap below the onset of continuum transitions.

For the  $\text{Cu}^{2+}$  ions in solution, a strong but broadened  $4p$  resonance is observed to occur above the continuum threshold. The 13 eV between this feature and the first peak for the  $\text{Cu}^{1+}$  ions is significantly greater than the 9-eV shift obtained from the calculation for the isolated ions due to removing one  $3d$  electron. At least part of the difference may be due to the excitonic binding energy for the  $\text{Cu}^{1+}$  ion. An extremely weak quadrupole-allowed  $1s \rightarrow 3d$  transition occurs 18 eV below the  $4p$  peak, in excellent agreement with the calculation. That the small pre-edge peak is predominantly due to a quadrupole transition has been demonstrated experimentally through a polarization-dependent study on a square planar  $\text{CuCl}_4^{2-}$  complex.<sup>40</sup>

One may notice that the  $\text{Cu}_2\text{O}$  spectrum has a bump in the same position as the  $4p$  resonance of the  $\text{Cu}^{2+}$  ions. However, as may be seen in Fig. 1 of our first paper,<sup>24</sup> the  $4p$  resonance is much stronger than the  $\text{Cu}_2\text{O}$  bump. We attribute the latter feature to fine structure occurring at the top of the absorption jump which overlaps with the  $\text{Cu}^{2+}$  peak by coincidence.

Cu  $K$ -edge XANES measurements on the  $\text{Cu}^{2+}$  compounds are presented in Fig. 2. For reference, the curve for the  $\text{Cu}^{2+}$  ions is plotted as a dashed line. In each case the overall shape, intensity, and position of the main peak agrees well with that of the  $\text{Cu}^{2+}$  ion; the position of the leading edge is especially consistent. Fine structure is seen to modulate the shape of the peak in the solid compounds, but the centroid is amazingly constant. At the foot of (approximately 10 eV below) the main peak in each of the compounds, an extra shoulder or peak is observed to which there is no analog in the solution. From *ab initio* self-consistent field and configuration interaction calculations on a hypothetical  $\text{CuCl}_2$  molecule, Bair and Goddard<sup>41</sup> found that such a feature corresponds to a  $1s \rightarrow 4p$  transition combined with the simultaneous "shake-down" transition of a high-energy ligand electron into the Cu  $3d$  hole. The screening of the core hole due to the charge transfer lowers the energy of the combined transitions relative to the unscreened excitation. Essentially identical interpretations have been obtained from two similar calculations.<sup>42,43</sup> The argument for this assignment is strengthened by the lack of a shake-down feature in the solution, where strong chemical bonding does not occur.

The edge for  $\text{CuFe}_2\text{O}_4$ , unlike the other edges in Fig. 2,

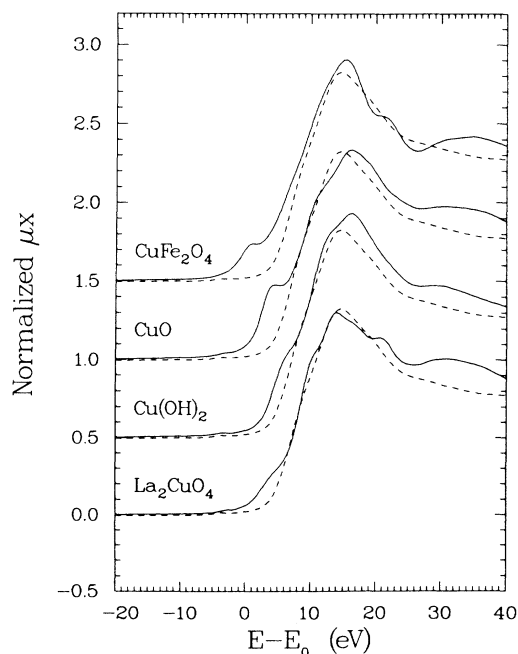


FIG. 2. Normalized XANES measured at the Cu  $K$  edge in several  $\text{Cu}^{2+}$  reference compounds. The dashed line in each case represents the edge for  $\text{Cu}^{2+}$  ions in solution. The curves have been shifted vertically for clarity.

exhibits a small peak at  $\sim 1$  eV, similar in position to the initial peak observed in the  $\text{Cu}^{1+}$  references. Identification of this peak with a small number of  $\text{Cu}^{1+}$  ions in tetrahedral sites is consistent with the x-ray diffraction results and theoretical expectations discussed earlier. Note that for this inhomogeneously mixed-valent system, the edge appears to be a simple superposition of 1+ and 2+ contributions.

The consistent peak position for the  $\text{Cu}^{2+}$  compounds and its large shift from the  $\text{Cu}^{1+}$  peaks suggests that the  $\text{Cu}^{2+}$  ions all have the same localized electronic configuration. If these systems were strongly covalent we would expect the edge and peak positions to shift around between the 1+ and 2+ extremes. The lack of such variation among the edges is consistent with essentially integral  $3d^{10}$  and  $3d^9$  configurations for the  $\text{Cu}^{1+}$  and  $\text{Cu}^{2+}$  ions, respectively. While a small amount of covalency may occur, the important point is that the effective copper configuration is the same in all of the 2+ reference systems. The somewhat surprising but general tendency of Cu ions to exhibit either  $\text{Cu}^{1+}$  or  $\text{Cu}^{2+}$  features is demonstrated by the work of Kau *et al.*<sup>44</sup> who measured Cu *K* edges in  $19\text{Cu}^{1+}$  and  $40\text{Cu}^{2+}$  (mostly organic) compounds with various ligands. The only compounds with "covalent" edge positions (between the extremes) contained sulfur ligands.

We have calculated that removing a second  $3d$  electron should result in a  $\sim 10$  eV peak shift in going from  $\text{Cu}^{2+}$  to  $\text{Cu}^{3+}$ , although we have presented no experimental results for a  $\text{Cu}^{3+}$  compound. Such a measurement has been presented for  $\text{KCuO}_2$  by Alp *et al.*,<sup>45</sup> who find that the  $4p$  peak shifts  $\sim 4$  eV relative to  $\text{CuO}$ . While this shift is less than what we expect for a true  $3d^8$  configuration, it demonstrates that a substantial peak shift does occur when Cu is oxidized beyond the 2+ state.

### C. $\text{La}_{2-x}(\text{Ba,Sr})_x\text{CuO}_{4-y}$

With some understanding of how to interpret Cu *K* near-edge structure, we now proceed to the samples of interest. Consider first the Cu *K* edge measured for  $\text{La}_2\text{CuO}_4$ , as shown in Fig. 2. It lines up extremely well with the  $\text{Cu}^{2+}$  reference edges, with good agreement in amplitude and position of the  $4p$  resonance, implying that the Cu ions in  $\text{La}_2\text{CuO}_4$  also have integral  $3d^9$  configurations. Placing firm error bars on this result is not easy since the fine structure makes it difficult to specify an exact edge or peak position. However, we note that displacing the observed edge by 1 eV, corresponding to a change of  $\sim 0.1$  electron, results in an obvious gap relative to the edge for  $\text{Cu}^{2+}$  ions in solution. The lack of any such gap suggests that the difference in  $3d$  occupation between the  $\text{La}_2\text{CuO}_4$  and the reference materials is much less than a tenth of an electron, and the overall consistency of the edge positions is strong circumstantial evidence for integral valence.

In the band-structure calculations for tetragonal  $\text{La}_2\text{CuO}_4$ ,<sup>15-17</sup> part of the  $3d$  hole on a copper atom is transferred to neighboring oxygen atoms due to hybridization, so that the average number of  $3d$  electrons is midway between 9 and 10. These calculations predict an edge po-

sition midway between the 1+ and 2+ standards, in sharp disagreement with the measurement. One might argue that the copper atoms have integral valences of 1+ and 2+ with an average corresponding to the net valence obtained from the band-structure calculations. However, if such a description were correct, we would expect to see a superposition of  $\text{Cu}^{1+}$  and  $\text{Cu}^{2+}$  edges of comparable step size which is clearly not observed.

Cu *K*-edge measurements as a function of Sr and Ba doping are plotted in Fig. 3. The measured edges are remarkably similar, with essentially no shift in the edge position due to doping. There are some very small shifts in the fine structure, but no qualitative changes. These results indicate that the number of copper  $3d$  holes does not change with doping. This point deserves special emphasis: Whether or not one is convinced that the Cu ions have an integral  $3d^9$  configuration, the data clearly show that the electron configuration on the copper does not change with doping. Edge measurements between 10 and 300 K on four of the samples indicate that there is no detectable temperature dependence of the near-edge structure.

To emphasize the connection between the bumps in the edge structure and the extended x-ray-absorption fine structure (EXAFS), we have fitted and subtracted a cubic spline through the data above and including the edge. The resulting interference functions  $\chi(k)$ , normalized to the edge step, are plotted in Fig. 4. In Fig. 4(a), the EXAFS measured at 10 K for the undoped sample and for Sr doped with  $x=0.15$ , corresponding to orthorhombic and tetragonal structures, respectively, are compared. (Actually, at this temperature the doped sample probably has an orthorhombic structure also, but with a much smaller distortion from the tetragonal phase than for the undoped one.<sup>46</sup>) One can see that there are small but clear shifts and changes in the fine structure at all values of  $k$ , the

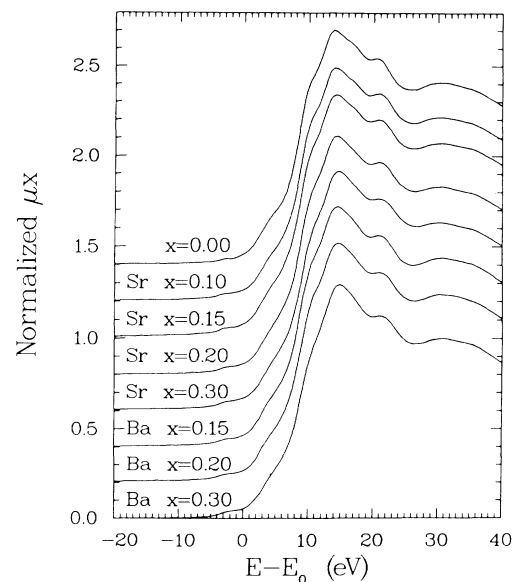


FIG. 3. Normalized XANES measured at the Cu *K* edge in  $\text{La}_{2-x}\text{A}_x\text{CuO}_{4-y}$  as a function of doping. The curves have been shifted vertically for clarity.

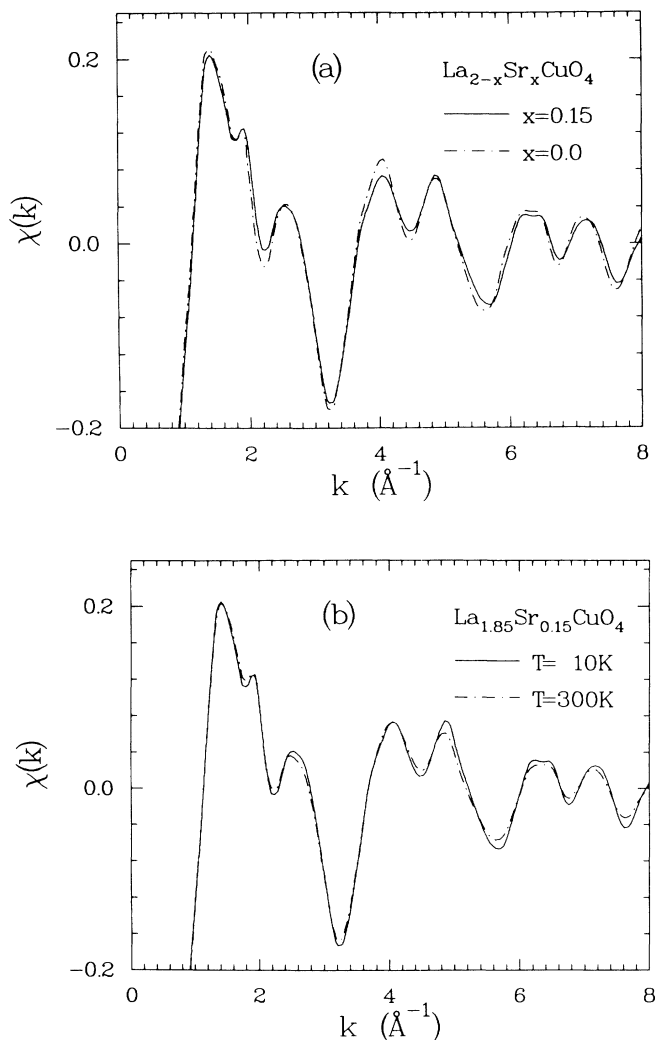


FIG. 4. Interference functions  $\chi(k)$  obtained from Cu  $K$  edge absorption measurements. (a) Comparison of data for  $\text{La}_2\text{CuO}_{4-y}$  and  $\text{La}_{1.85}\text{Sr}_{0.15}\text{CuO}_{4-y}$  measured at 10 K. (b) Comparison of data for  $\text{La}_{1.85}\text{Sr}_{0.15}\text{CuO}_{4-y}$  at 10 and 300 K.

photoelectron wave vector. These small changes are to be expected due to the slight difference between the structures. The temperature dependence of the fine structure for the Sr-doped sample is illustrated in Fig. 4(b). The decrease in amplitude of the oscillations with increasing temperature is consistent with the damping of scattering contributions due to lattice vibrations. We believe that the structure and temperature dependence of the fine structure in the region of the  $4p$  peak region ( $1-2 \text{\AA}^{-1}$ ) demonstrate that these oscillations are due to scattering rather than atomlike effects.

In order to appreciate the significance of the doping results, we must first consider the effects anticipated when Sr or Ba is substituted for La. Lanthanum has a formal valence of  $3+$ , while the alkaline earths are  $2+$ . The band-structure calculations indicate that the La, Ba, and Sr atomic orbital contributions to the valence bands are

relatively small, and so the actual valence configurations of these ions should be close to their formal charges. For each trivalent ion which is replaced by a divalent atom, one less electron is contributed to the valence bands. Since the net charge per formula unit must be zero, this effect is sometimes interpreted as implying that for each dopant ion, one copper atom must change its valence from  $2+$  to  $3+$ .

It is well established that oxygen vacancies are quite common in the  $\text{La}_{2-x}(\text{Ba},\text{Sr})_x\text{CuO}_{4-y}$  system.<sup>47</sup> If  $y$  were exactly equal to  $x/2$ , then all of the copper atoms could remain  $2+$ . It is observed,<sup>48</sup> however, that these oxides can be prepared with  $y \ll x/2$ , so that the number of valence electrons does decrease with  $x$ . It has also been found that heating the oxide superconductors in vacuum so as to drive off oxygen can cause virtual elimination of their superconducting properties.<sup>49</sup> It is apparent that a valence electron deficiency is important for superconductivity, while oxygen vacancies have a negative effect on it.

The generally good superconducting properties of our samples suggest that the number of oxygen vacancies must be relatively small. We wish to consider, then, how the valence electron deficiency due to doping may manifest itself. In the band-structure approach, the simplest extrapolation is to assume that the electron energy bands are fixed and that the Fermi energy drops smoothly with the decreasing number of valence electrons. Such a model implies that both the numbers of Cu  $3d_{x^2-y^2}$  and O  $2p_{x,y}$  electrons decrease with doping. Assuming that the decrease is shared equally among one copper and two oxygen atoms (with no vacancies), a change in  $3d$  occupation of 0.1 electron would be expected for  $x=0.3$ . Such a change should correspond to an edge shift of  $\sim 1$  eV, which is not observed. From calculations on both  $\text{La}_2\text{CuO}_4$  and (hypothetical)  $\text{LaBaCuO}_4$ , Pickett, Krakauer, Papaconstantopoulos, and Boyer<sup>17</sup> have found that the rigid-band picture is not quite correct. A greater part of the change appears to be taken up by the oxygen atoms, a result consistent with our measurements.

At the other extreme, one might consider the Cu  $3d$  electrons to be localized rather than itinerant. In that case, the number of  $3d$  electrons on an atom would be integral rather than continuously variable. If the Mott-Hubbard  $d-d$  correlation energy  $U$  is not too great, divalent doping could cause some copper atoms to convert from  $3d^9$  to  $3d^8$ . Assuming that the change in valence charge is entirely accounted for in this manner, we would expect that for  $x=0.3$  the  $\text{Cu}^{2+}$  edge features should be reduced by 30% and a  $\text{Cu}^{3+}$  edge should appear shifted by  $\sim 10$  eV to higher energy. A systematic trend toward this limit should be observed for intermediate  $x$ . There is no evidence for such a trend in the data of Fig. 3.

Alp *et al.*<sup>45</sup> have obtained experimental results quite similar to ours for the Cu  $K$  edge in  $\text{La}_{2-x}(\text{Ba},\text{Sr})_x\text{CuO}_{4-y}$  over the same range of  $x$ . They have, however, come up with a somewhat different interpretation of the data. They interpret the bump at  $\sim 21$  eV as being due to the superposition of an edge corresponding to  $\text{Cu}^{3+}$  on top of the  $\text{Cu}^{2+}$  edge. In support of this assignment, the results of cluster calculations are presented. It is stated that the *ab initio* calculations indicate near degeneracy of two



electronic ground states “nominally representing the two valence states of Cu.”<sup>45</sup> However, the effective Cu 3*d* occupancy of one of the ground states is found to be 9.39, with the occupancy of the other smaller by 0.3 electrons. We would say that both of these states correspond to copper valences between 2+ and 1+, not 2+ and 3+. Furthermore, our empirical comparison with reference compounds strongly indicates that the Cu 3*d* occupancy is 9.0 and not 9.4.

Also presented as evidence for the alleged presence of Cu<sup>3+</sup> are multiple-scattered-wave (MSW) calculations of the x-ray-absorption cross section. The lack of a calculated feature corresponding to the 21-eV bump is cited in support of the Cu<sup>3+</sup> assignment. We wish to point out, however, that to our knowledge, MSW calculations performed to date<sup>50</sup> have generally not achieved much better than qualitative agreement with experiment and that such discrepancies are common. We also refer to Fig. 4, in which the fine-structure-like behavior of the 21-eV bump is demonstrated. Finally, no explanation for the approximately constant intensity of the feature with doping is given. If two valences are present, one would expect to see some variation in the relative amounts with doping as discussed above.

Summarizing our findings to this point, our Cu *K*-edge measurements indicate that Cu has a 3*d*<sup>9</sup> configuration in La<sub>2-x</sub>(Ba,Sr)<sub>x</sub>CuO<sub>4-y</sub> independent of *x* for *x*=0 to 0.3. No evidence is found for either nonintegral valence, as expected for itinerant 3*d* electrons, or for mixed valence. Our results suggest that the 3*d* electrons are highly localized due to a large Coulomb correlation energy. As will be discussed later, we interpret measurements on the La L<sub>2,3</sub> edges as indicating that the decrease in valence charge due to doping is completely compensated by the creation of holes in the O 2*p* band. We will now discuss how such holes affect the Cu *K*-edge XANES.

As previously discussed, band-structure calculations find that the top valence band involves an antibonding combination of Cu 3*d*<sub>x<sup>2</sup>-y<sup>2</sup></sub> and O 2*p*<sub>x,y</sub> states. Although we do not observe the Cu 3*d* hybridization, if we nevertheless assume that the top valence band consists of O 2*p* states combined to have *d* symmetry with respect to the copper sites, then any unoccupied states at the top of the band will have little effect on dipole transitions at the Cu *K* edge. These states may, however, contribute to quadrupole transitions.

To enhance the quadrupole and “shakedown” features, the measured edge for Cu<sup>2+</sup> ions in solution (with the quadrupole peak removed by interpolation) was subtracted from the edges for La<sub>2-x</sub>Sr<sub>x</sub>CuO<sub>4-y</sub>, and the results are shown in Fig. 5. The quadrupole feature is observed to increase with *x* and shift to higher energy. This result is consistent with an increasing number of O 2*p* holes having *d* symmetry with respect to the Cu site. The decrease in intensity of the “shake-down” peak could also be due to a reduction in the number of high-energy O 2*p* electrons.

Stern<sup>51</sup> has pointed out that in order for the final state of a quadrupole transition to have a large overlap with the Cu 1*s* core level, it must by definition be a Cu *d* state. This argument, together with the previous discussion, leads to the conclusion that the number of Cu *d* final

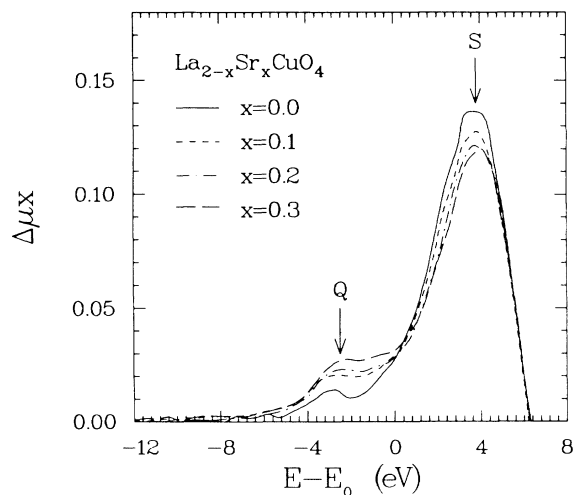


FIG. 5. Near-edge structure measured at the Cu *K* edge in La<sub>2-x</sub>Sr<sub>x</sub>CuO<sub>4-y</sub> after subtraction of a reference edge as discussed in the text. The feature labeled *Q* is the quadrupole peak and the feature labeled *S* is the “shake-down” peak.

states is increasing with doping, in apparent contradiction to our previous interpretation of the dipole transition features. We believe, however, that the two conclusions can be reconciled in the following way.

While the Cu ions appear to have an essentially 3*d*<sup>9</sup> configuration, a small but finite hybridization with the O 2*p* states probably exists. The core hole due to x-ray absorption is a significant perturbation on the system, and in its presence the local hybridization may increase. A *d*-symmetry combination of O 2*p* states combined with the Cu 3*d* hole, when occupied by the photoelectron, is a low-energy state because it screens the core-hole well. The core-hole-induced hybridization then increases the effective number of Cu *d* holes and, hence, results in an increased amplitude for the quadrupole feature. Because of the lower energy of the filled hybridized state plus core-hole combination, an unusual type of core-hole screening may occur in these oxides. An O 2*p* hole may move to a site neighboring the core-hole location because when occupied by the photoelectron the total energy is lower than that of an isolated, empty hole plus the photoelectron.

We have indicated that the core hole perturbs the system. Can we actually measure the unperturbed Cu 3*d* configuration in the presence of the core hole? The 4*p* resonance is due to the presence of the core hole; it would not be as strong if the core hole were well screened by mobile conduction electrons. The Cu 4*p* state is not expected to hybridize strongly with any oxygen states and so the 1*s* → 4*p* transition should be atomiclike. The Cu 3*d* electrons help to screen the initial and final states. Increased hybridization of the filled O 2*p* states with the Cu 3*d* hole can decrease the final-state energy by transferring an electron from the oxygen to the copper. This charge relaxation results in the readily identified shake-down feature previously discussed. The position of the 4*p* resonance feature should therefore be correlated with the unperturbed *d* configuration as we have assumed.



#### IV. La $L$ EDGES

According to the dipole selection rule,  $L_{2,3}$  edges involve transitions from  $2p$  to  $d$ -symmetry final states. Transitions from  $p$  to  $s$  symmetry are also allowed, but have a cross section approximately 50 times smaller than  $p$  to  $d$  and can be ignored in the near-edge region.<sup>52,53</sup> An atom with a large density of unoccupied  $d$  states just above the Fermi energy will exhibit a large absorption peak commonly referred to as a “white line” at the  $L_3$  and  $L_2$  edges. The area under a white line is related to the number of  $d$  holes.

The  $L_3$  and  $L_2$  edges are generally spin-orbit split and correspond to  $2p_{3/2}$  and  $2p_{1/2}$  initial states, respectively. A  $\text{La}^{3+}$  ion should have 10 empty  $5d$  states split between total angular momenta of  $\frac{5}{2}$  and  $\frac{3}{2}$ . It has been shown<sup>54</sup> that the areas under the white lines,  $A_{L_2}$  and  $A_{L_3}$ , at the  $L_{2,3}$  edges can be expressed in terms of the number of  $d$  holes as

$$A_{L_3} = \frac{1}{60} (6 |R_{d_{5/2}}^{2p_{3/2}}|^2 h_{5/2} + |R_{d_{3/2}}^{2p_{3/2}}|^2 h_{3/2}), \quad (1)$$

$$A_{L_2} = \frac{5}{60} |R_{d_{3/2}}^{2p_{1/2}}|^2 h_{3/2}, \quad (2)$$

where  $R_{l_j}^{n'l'j'}$  is the radial dipole matrix element between initial and final states having quantum numbers  $n', l', j'$  and  $l, j$ , respectively, and  $h_j$  is the number of  $d$  holes with total angular momentum  $j$ .

Our results for the La  $L_3$  edge in  $\text{La}_{2-x}\text{Sr}_x\text{CuO}_{4-y}$  have been shown previously.<sup>24</sup> The white line is observed to increase in height and area with increasing  $x$ . Similar trends have been observed for Ba doping and at the  $L_2$  edge for both Sr and Ba doping. Doping clearly causes an increase in the number of unoccupied states having  $d$  symmetry with respect to the La site. A semiquantitative analysis of the data is attempted here.

The strong peak due to transitions to empty, localized  $d$  states overlaps with a steplike absorption involving delocalized final states. In order to isolate the  $d$  contribution one must have some way of modeling the background absorption, and several approaches have been discussed in the literature.<sup>55,56</sup> We have chosen to simulate the normalized absorption step  $\mu_s(E)x$  with an arctangent function,<sup>57</sup>

$$\mu_s(E)x = \frac{1}{2} - \frac{1}{\pi} \tan^{-1} \left( \frac{E_s - E}{\Gamma/2} \right), \quad (3)$$

whose position  $E_s$  and width  $\Gamma$  were chosen to satisfy the arbitrary criterion that the residual peak appear symmetric. The midpoint of the step was chosen to be approximately 2 eV above the peak center, and a width  $\Gamma = 6$  eV was found to give good results. The residual peaks obtained at the La  $L_3$  edge for several concentrations of Sr are shown in Fig. 6. The area of a peak was obtained by numerical integration from 15 eV below to 15 eV above the peak center.

As we are interested in the change in the number of empty  $d$  states with doping, it is convenient to discuss the white line areas in the form  $[A(x) - A(0)]/A(0)$ , where  $A(x)$  is the peak area for  $x$  amount of dopant. The results for both Sr and Ba doping, measured at the  $L_2$  and  $L_3$  edges, are summarized in Fig. 7. Shifting the step po-

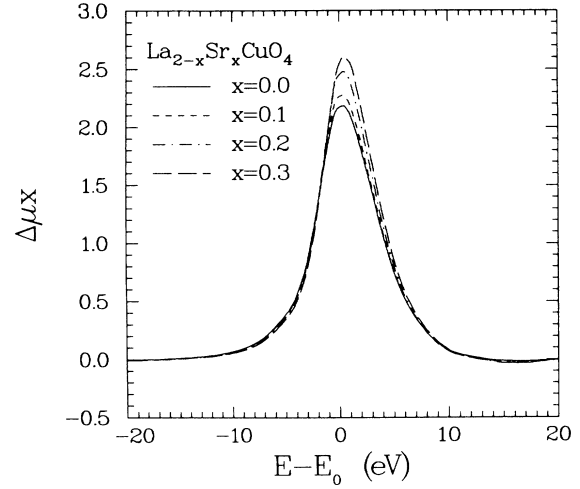


FIG. 6 Residual white-line peaks obtained at the La  $L_3$  edge in  $\text{La}_{2-x}\text{Sr}_x\text{CuO}_{4-y}$  after subtraction of an arctangent function as described in the text;  $E_0 = 5488$  eV.

sition  $E_s$  by 2 eV cause a change of  $\sim 10\%$  in the relative area changes. The  $L_2$  and  $L_3$  areas give similar results, and the Sr and Ba compounds follow the same trend. The scatter among samples is probably due to variations in sample quality and oxygen content. The relative area increase is 6%–9% for the higher doping levels. If we assume that there are no variations in the radial dipole matrix elements and that there are ten  $5d$  holes in  $\text{La}_2\text{CuO}_4$ , then the white-line area changes indicate an increase of 0.6–0.9  $d$ -symmetry holes per lanthanum atom for the highly doped samples.

The La  $L_{2,3}$  edge results are qualitatively consistent with the decrease in the number of valence electrons expected due to replacing  $\text{La}^{3+}$  by  $\text{Sr}^{2+}$  or  $\text{Ba}^{2+}$ . The holes which are opened by doping could be either La  $5d$  states

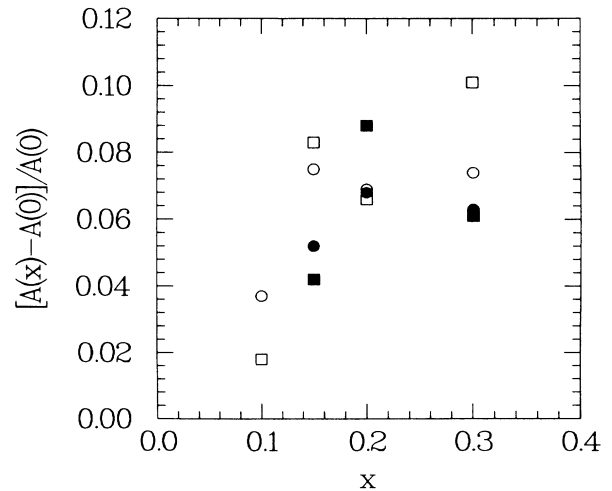


FIG. 7. Relative white-line area change,  $[A(x) - A(0)]/A(0)$ , in  $\text{La}_{2-x}\text{A}_x\text{CuO}_{4-y}$  as a function of dopant level  $x$ . Open symbols,  $A = \text{Sr}$ ; solid symbols,  $A = \text{Ba}$ ; squares, La  $L_3$  edge; circles, La  $L_2$  edge.

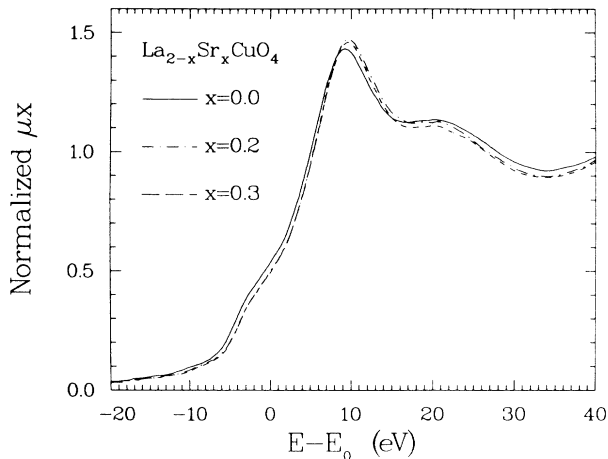


FIG. 8. Edge structure measured at the La  $L_1$  edge in  $\text{La}_{2-x}\text{Sr}_x\text{CuO}_{4-y}$  for several values of  $x$ .

or  $d$ -symmetric linear combinations of O  $2p$  states at the top of the valence band. The former possibility requires that the La  $5d$  band dip below the Fermi energy in the undoped material, as has been suggested by Emery<sup>23</sup> to explain observations<sup>58</sup> of superconductivity in  $\text{La}_2\text{CuO}_4$  and the pressure dependence of  $T_c$ .<sup>4</sup> It seems likely, though, that at least part of the white line increase is due to holes in O  $2p$  states. Linear combinations of such states having  $d$  symmetry with respect to the Cu sites will also have a  $d$ -symmetric component about a La position. Although the energy calibration is much less reliable than for the Cu  $K$  edge, the lack of any substantial edge shift is more consistent with the creation of O  $2p$  holes rather than decreasing occupation of La  $5d$  states.

Ignoring defects, one would expect the number of holes per lanthanum atom to have a maximum of  $\sim 0.15$  for  $x=0.3$ ; taking defects into account would probably decrease the estimate. This number is roughly a factor of 5 less than that estimated from the white-line areas. The discrepancy may be due to variations in the radial dipole-matrix elements resulting from changes in screening. Another possibility is that an unusual screening effect could occur in which a La core hole could attract on O  $2p$  hole because filling such a hole would localize the photoelectron and help to screen the core hole, as discussed with respect to the quadrupole feature at the Cu  $K$  edge. Such a mechanism might lead to a larger effective O  $2p$  hole density.

For completeness, several examples of the La  $L_1$  edge are shown in Fig. 8, corresponding to different doping levels. Because the  $L_1$  edge is superimposed on the fine structure extending above the  $L_2$  edge, we are hesitant to speculate on the significance of the small changes that occur with doping. A clear-cut interpretation of the main features at this edge is also lacking.

## V. DISCUSSION AND SUMMARY

The measurements at the Cu  $K$  edge in  $\text{La}_{2-x}(\text{Ba},\text{Sr})_x\text{CuO}_{4-y}$  show that the copper atoms have

a  $3d^9$  configuration independent of  $x$ . No evidence for mixed-valent copper is observed. The changes in the quadrupole feature at the Cu edge and the variations in the white-line intensity at the La  $L_{2,3}$  edges indicate that reduction in valence charge due to doping results in holes in the O  $2p$  band. These holes have  $d$  symmetry with respect to the Cu and La sites. Presumably the oxygen holes carry the charge in the superconducting state. Regardless of the exact electronic configuration of the copper, the important result is that doping appears to put holes in the O  $2p$  band but does not affect the Cu.

These conclusions are supported by at least two other experiments. The discovery<sup>59-64</sup> of antiferromagnetism in  $\text{La}_2\text{CuO}_{4-y}$  indicates that correlation effects are quite important in this system and is consistent with our determination of a  $3d^9$  configuration for the copper ions. Hall-effect measurements<sup>65</sup> in  $\text{La}_{2-x}\text{Sr}_x\text{CuO}_{4-y}$  indicate that the charge carriers are holes and that for  $x \leq 0.15$  there is one hole per Sr atom. As  $x$  increases to larger values the Hall constant drops rapidly, deviating from this trend. The small- $x$  behavior is consistent with our observation of O  $2p$  holes and with the number of holes expected due to doping (with defects ignored).

From our present results together with our EXAFS study,<sup>24</sup> we believe that electron-pairing models based on electron-electron correlations rather than electron-phonon interactions are on the right track. While our observations give no direct insight into the superconducting mechanism, they do help to define the relevant parameters that must be included in models for superconductivity in the high- $T_c$  oxides. With this in mind, we offer the following comments on several proposed theories in terms of our current understanding of these rapidly evolving ideas.

The band-structure calculations<sup>15-17</sup> for  $\text{La}_2\text{CuO}_4$  predict that the Cu  $3d$  hole is shared between a copper atom and its oxygen neighbors. The discrepancy between this prediction and our observations suggests that the calculations underestimate the correlation energy. It also casts considerable doubt on the calculations of the electron-phonon interaction<sup>66</sup> based on the band-structure results.

The presence of only a single valence of copper, independent of doping, is strong evidence against any model for electron pairing that requires mixed valence, such as the theory of Varma *et al.*<sup>22</sup> Our results, together with the observation of antiferromagnetism and the Hall effect results, indicate that electron correlation effects are quite important in the  $\text{La}_{2-x}(\text{Ba},\text{Sr})_x\text{CuO}_{4-y}$  system. The strong Coulomb correlation energy for Cu  $3d$  electrons causes dopant-induced holes to spend most of their time on the oxygen sites. Anderson's RVB model<sup>18</sup> takes the correlation into account, but it is not clear to us that the theory is consistent with holes predominately on the oxygen rather than the copper.

The theory which is most clearly consistent with the x-ray-absorption results is that due to Emery.<sup>23</sup> His extended-Hubbard model approach shows that it is energetically reasonable for the Cu ions to have a  $3d^9$  configuration. The relatively large correlation energy for  $d$  states, which is responsible for the integral valence of the copper, can also cause holes introduced by doping to end up on the oxygen sites. The model gains further cred-

ibility from its prediction of antiferromagnetism in  $\text{La}_2\text{CuO}_4$ .

The recent discovery<sup>58</sup> of superconductivity in  $\text{La}_2\text{CuO}_4$  (annealed in high-pressure  $\text{O}_2$ ) requires some discussion. According to Emery's model, superconductivity is due to pairing of O  $2p$  holes, and such holes do not exist in the simplest ionic picture of  $\text{La}_2\text{CuO}_4$ . However, holes could be formed if the La  $5d$  conduction-band dips below the Fermi energy and soaks up some valence electrons.<sup>23</sup> Another possibility involves the presence of structural defects.<sup>67</sup> The structure of  $\text{La}_2\text{CuO}_4$  can be viewed as a stacking of two layers of LaO alternating with a  $\text{CuO}_2$  layer. A general formula for such layered structures can be written as  $(\text{LaO})_{n+1}(\text{CuO}_2)_n$ , where  $n=1$  for  $\text{La}_2\text{CuO}_4$ . The LaO layers tend to donate electrons while the  $\text{CuO}_2$  layers accept charge, and if excess  $\text{CuO}_2$  layers are present, O  $2p$  holes should occur. It has been demonstrated<sup>68</sup> that  $(\text{LaO})_{n+1}(\text{CuO}_2)_n$  with  $n=1, 2, 3, 4$ , and greater can be formed, especially as isolated lamellae in a disordered crystal. (The high- $T_c$   $\text{YBa}_2\text{Cu}_3\text{O}_{9-y}$  compound appears to have a related structure containing a greater fraction of  $\text{CuO}_2$  planes.<sup>69,70</sup>) Presumably extra

$\text{CuO}_2$  layers could occur in  $\text{La}_2\text{CuO}_4$  as defects and provide sufficient O holes to explain the superconductivity. It is significant that antiferromagnetism occurs only in samples with a nonstoichiometric concentration of oxygen.<sup>59</sup> The oxygen defects leave behind electrons which fill any oxygen holes, resulting in the half-filled band condition for which antiferromagnetism is expected.<sup>23</sup>

#### ACKNOWLEDGMENTS

One of us (J.M.T.) gratefully acknowledges the guidance of J. W. Davenport in performing the atomic calculations and wishes to thank him and V. J. Emery for many insightful discussions on theory. A discussion with H. Krakauer and the help of H. Isaacs in preparing a sample are also appreciated. The authors would especially like to thank M. Suenaga for performing the susceptibility measurements. This work was performed on beam line X-11 at the National Synchrotron Light Source and is supported by the U.S. Department of Energy under Contracts No. DE-AC02-76CH00016 and No. DE-AS05-80-ER10742.

- <sup>1</sup>J. G. Bednorz and K. A. Müller, *Z. Phys. B* **64**, 189 (1986).
- <sup>2</sup>S. Uchida, H. Takagi, K. Kitazawa, and S. Tanaka, *Jpn. J. Appl. Phys. Lett.* **26**, L1 (1987).
- <sup>3</sup>H. Takagi, S. Uchida, K. Kitawawa, and S. Tanaka, *Jpn. J. Appl. Phys. Lett.* **26**, L123 (1987).
- <sup>4</sup>C. W. Chu, P. H. Hor, R. L. Meng, L. Gao, Z. J. Huang, and Y. Q. Wang, *Phys. Rev. Lett.* **58**, 405 (1987).
- <sup>5</sup>R. J. Cava, R. B. van Dover, B. Batlogg, and E. A. Rietman, *Phys. Rev. Lett.* **58**, 408 (1987).
- <sup>6</sup>J. G. Bednorz, K. A. Müller, and M. Takashige, *Science* **236**, 73 (1987).
- <sup>7</sup>M. Sato, S. Hosoya, S. Shamoto, M. Onoda, K. Imaeda, and H. Inokuchi, *Solid State Commun.* **62**, 85 (1987).
- <sup>8</sup>M. K. Wu, J. R. Ashburn, C. U. Torng, P. H. Hor, R. L. Meng, L. Gao, Z. J. Huang, Y. Q. Wang, and C. W. Chu, *Phys. Rev. Lett.* **58**, 908 (1987).
- <sup>9</sup>P. H. Hor, L. Gao, R. L. Meng, Z. J. Huang, Y. Q. Wang, K. Forster, J. Vassiliou, C. W. Chu, M. K. Wu, J. R. Ashburn, and C. J. Torng, *Phys. Rev. Lett.* **58**, 911 (1987).
- <sup>10</sup>R. J. Cava, B. Batlogg, R. B. van Dover, D. W. Murphy, S. Sunshine, T. Siegrist, J. P. Remeika, E. A. Rietman, S. Zahurak, and G. P. Espinosa, *Phys. Rev. Lett.* **58**, 1676 (1987).
- <sup>11</sup>D. W. Murphy, S. Sunshine, R. B. van Dover, R. J. Cava, B. Batlogg, S. M. Zahurak, and L. F. Schneemeyer, *Phys. Rev. Lett.* **58**, 1888 (1987).
- <sup>12</sup>P. H. Hor, R. L. Meng, Y. Q. Wang, L. Gao, Z. J. Huang, J. Bechtold, K. Forster, and C. W. Chu, *Phys. Rev. Lett.* **58**, 1891 (1987).
- <sup>13</sup>J. D. Jorgensen, H.-B. Schüttler, D. G. Hinks, D. W. Capone II, K. Zhang, M. B. Brodsky, and D. J. Scalapino, *Phys. Rev. Lett.* **58**, 1024 (1987).
- <sup>14</sup>V. B. Grande, Hk. Müller-Buschbaum, and M. Schweizer, *Z. Anorg. Allg. Chem.* **428**, 120 (1977).
- <sup>15</sup>L. F. Mattheiss, *Phys. Rev. Lett.* **58**, 1028 (1987).
- <sup>16</sup>J. Yu, A. J. Freeman, and J.-H. Xu, *Phys. Rev. Lett.* **58**, 1035 (1987).
- <sup>17</sup>W. E. Pickett, H. Krakauer, D. A. Papaconstantopoulos, and L. L. Boyer, *Phys. Rev. B* **35**, 7252 (1987).
- <sup>18</sup>P. W. Anderson, *Science* **235**, 1196 (1987).
- <sup>19</sup>G. Baskaran, Z. Zou, and P. W. Anderson (unpublished).
- <sup>20</sup>S. A. Kivelson, D. S. Rokhsar, and J. P. Stehna, *Phys. Rev. B* **35**, 8865 (1987).
- <sup>21</sup>D. H. Lee and J. Ihm, *Solid State Commun.* **62**, 811 (1987).
- <sup>22</sup>C. M. Varma, S. Schmitt-Rink, and E. Abrahams, *Solid State Commun.* **62**, 681 (1987).
- <sup>23</sup>V. J. Emery, *Phys. Rev. Lett.* **58**, 2794 (1987).
- <sup>24</sup>J. M. Tranquada, S. M. Heald, A. R. Moodenbaugh, and M. Suenaga, *Phys. Rev. B* **35**, 7187 (1987).
- <sup>25</sup>K. A. Müller, M. Takashige, and J. B. Bednorz, *Phys. Rev. Lett.* **58**, 1143 (1987).
- <sup>26</sup>K. Alder, B. Baur, and U. Raff, *Helv. Phys. Acta* **45**, 765 (1972).
- <sup>27</sup>Relativistic calculations of the total energy of an atom in different configurations were performed using a computer program kindly provided by J. W. Davenport. Exchange and correlation were included with the local density approximation of Hedin and Lundquist. For details, see J. W. Davenport, M. Weinert, and R. E. Watson, *Phys. Rev. B* **32**, 4876 (1985); L. Hedin and B. I. Lundquist, *J. Phys. C* **4**, 2064 (1971).
- <sup>28</sup>N. N. Efremova, L. D. Finkel'shtein, N. D. Samsonova, and S. A. Nemnonov, *Bull Acad. Sci. USSR, Phys. Ser.* **40**, 170 (1976).
- <sup>29</sup>G. Bunker and E. A. Stern, *Phys. Rev. Lett.* **52**, 1990 (1984).
- <sup>30</sup>L. Kleinman and K. Mednick, *Phys. Rev. B* **21**, 1549 (1980).
- <sup>31</sup>J. B. Goodenough, in *Progress in Solid State Chemistry*, edited by H. Reiss (Pergamon, Oxford, 1971), Vol. 5, p. 145.
- <sup>32</sup>A. A. Ghani, S. A. Mazen, and A. H. Ashour, *Phys. Status Solidi (a)* **84**, 337 (1984).
- <sup>33</sup>P. Lagarde, A. Fontaine, D. Raoux, A. Sadoc, and P. Migliardo, *J. Chem. Phys.* **72**, 3061 (1980).
- <sup>34</sup>J. Garcia, A. Bianconi, M. Benfatto, and C. R. Natoli, *J. Phys. (Paris) Colloq.* **47**, C8-49 (1986).
- <sup>35</sup>H. Ohnishi and T. Teranishi, *J. Phys. Soc. Jpn.* **16**, 35 (1961).
- <sup>36</sup>N. Nanba, *J. Appl. Phys.* **49**, 2950 (1978).

- <sup>37</sup>J. E. Müller and W. L. Schaich, *Phys. Rev. B* **27**, 6489 (1983).
- <sup>38</sup>S. L. Hulbert, B. A. Bunker, F. C. Brown, and P. Pianetta, *Phys. Rev. B* **30**, 2120 (1984).
- <sup>39</sup>J. Robertson, *Phys. Rev. B* **28**, 3378 (1983).
- <sup>40</sup>J. E. Hahn, R. A. Scott, K. O. Hodgson, S. Doniach, S. R. Desjardins, and E. I. Solomon, *Chem Phys. Lett.* **88**, 595 (1982).
- <sup>41</sup>R. A. Bair and W. A. Goddard III, *Phys. Rev. B* **22**, 2767 (1980).
- <sup>42</sup>N. Kosugi, T. Yokoyama, K. Asakura, and H. Kuroda, *Chem. Phys.* **91**, 249 (1984).
- <sup>43</sup>T. A. Smith, J. E. Penner-Hahn, M. A. Berding, S. Doniach, and K. O. Hodgson, *J. Am. Chem. Soc.* **107**, 5945 (1985).
- <sup>44</sup>L.-S. Kau, D. J. Spira-Solomon, J. E. Penner-Hahn, K. O. Hodgson, and E. I. Solomon, *J. Am. Chem. Soc.* (to be published).
- <sup>45</sup>E. E. Alp, G. K. Shenoy, D. G. Hinks, D. W. Capone II, L. Soderholm, H.-B. Schüttler, J. Guo, D. E. Ellis, P. A. Montano, and M. Ramanathan, *Phys. Rev. B* **35**, 7199 (1987).
- <sup>46</sup>R. M. Fleming, B. Batlogg, R. J. Cava, and E. A. Rietman, *Phys. Rev. B* **35**, 7191 (1987).
- <sup>47</sup>C. Michel and B. Raveau, *Rev. Chim. Miner.* **21**, 407 (1984).
- <sup>48</sup>N. Nguyen, J. Chaoisnet, M. Hervieu, and B. Raveau, *J. Solid State Chem.* **39**, 120 (1981).
- <sup>49</sup>J. M. Tarascon, L. H. Greene, W. R. McKinnon, G. W. Hall, and T. H. Geballe, *Science* **235**, 1373 (1987).
- <sup>50</sup>See, for example, Ref. 43, and references therein.
- <sup>51</sup>E. A. Stern (private communication).
- <sup>52</sup>B.-K. Teo and P. A. Lee, *J. Am. Chem. Soc.* **101**, 2815 (1979).
- <sup>53</sup>S. M. Heald and E. A. Stern, *Phys. Rev. B* **16**, 5549 (1977).
- <sup>54</sup>L. F. Mattheiss and R. E. Dietz, *Phys. Rev. B* **22**, 1663 (1980).
- <sup>55</sup>F. W. Lytle, *J. Catal.* **43**, 376 (1976).
- <sup>56</sup>A. N. Mansour, J. W. Cook, and D. E. Sayers, *J. Phys. Chem.* **88**, 2330 (1984).
- <sup>57</sup>F. K. Richtmeyer, S. W. Barnes, and E. Ramberg, *Phys. Rev.* **46**, 843 (1934).
- <sup>58</sup>J. Beille, R. Cabanel, C. Chaillout, B. Chevallier, G. Demazeau, F. Deslanders, J. Etorneau, P. Lejay, C. Michel, J. Provost, B. Raveau, A. Sulpice, J.-L. Tholence, and R. Tournier (unpublished).
- <sup>59</sup>D. Vaknin, S. K. Sinha, D. E. Moncton, D. C. Johnston, J. Newsam, C. R. Safinya, and H. E. King, Jr., *Phys. Rev. Lett.* **58**, 2802 (1987).
- <sup>60</sup>R. L. Greene, H. Maletta, T. S. Plaskett, J. G. Bednorz, and K. A. Müller, *Solid State Commun.* **63**, 379 (1987).
- <sup>61</sup>S. Mitsuda, G. Shirane, S. K. Sinha, D. C. Johnston, M. A. Alvarez, D. Vaknin, and D. E. Moncton, *Phys. Rev. B* **36**, 822 (1987).
- <sup>62</sup>T. Freltoft, J. E. Fischer, G. Shirane, D. E. Moncton, S. K. Sinha, D. Vaknin, J. P. Remeika, A. S. Cooper, and D. Harshman, *Phys. Rev. B* **36**, 826 (1987).
- <sup>63</sup>B. X. Yang, S. Mitsuda, G. Shirane, Y. Yamaguchi, H. Yamaguchi, and Y. Syono, *J. Phys. Soc. Jpn.* **56**, 2283 (1987).
- <sup>64</sup>D. C. Johnston, J. P. Stokes, D. P. Goshorn, and J. T. Lewandowski (unpublished).
- <sup>65</sup>N. P. Ong, Z. Z. Wang, J. Clayhold, J. M. Tarascon, L. H. Greene, and W. R. McKinnon, *Phys. Rev. B* **35**, 8807 (1987).
- <sup>66</sup>W. Weber, *Phys. Rev. Lett.* **58**, 1371 (1987).
- <sup>67</sup>V. J. Emery (private communication).
- <sup>68</sup>A. H. Davies and R. J. D. Tilley, *Nature* **326**, 859 (1987).
- <sup>69</sup>M. A. Beno, L. Soderholm, D. W. Capone II, D. G. Hinks, J. D. Jorgensen, J. D. Grace, I. K. Schuller, C. U. Serge, and K. Zhang, *Appl. Phys. Lett.* **51**, 57 (1987).
- <sup>70</sup>D. E. Cox, A. R. Moodenbaugh, J. J. Hurst, and R. H. Jones (unpublished).